Journal of Materials Chemistry C

Accepted Manuscript

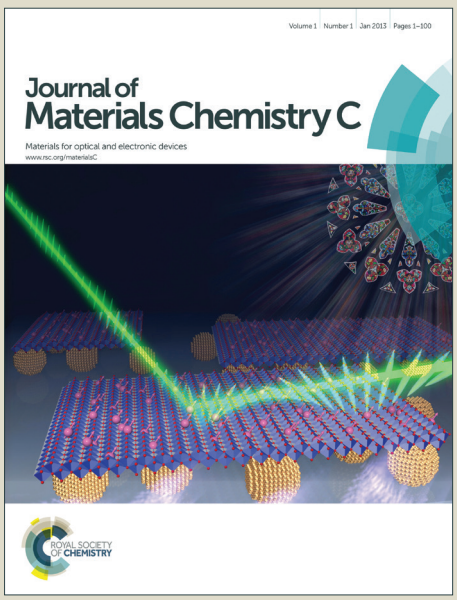

ROYAL SOCIETY OF CHEMISTRY

www.rsc.org/materialsC

Mesoporous TiO_2 Films with Regularly Aligned Slit-like Nanovoids

Hirokatsu Miyata,[1]* Yuta Fukushima,[2] Yosuke Kanno,[2] Saeko Hayase,[2] Shintaro Hara,[2] Masatoshi Watanabe,[1] Shin Kitamura,[1] Masahiko Takahashi[1] and Kazuyuki Kuroda[2, 3]*

1. Corporate R&D Headquarters, Canon Inc., 3-30-2 Shimomaruko, Ohta-ku, Tokyo 146-8501, Japan

2. Department of Applied Chemistry, Waseda University, 3-4-1 Ohkubo, Shinjuku-ku, Tokyo 169-8555, Japan

3. Kagami Memorial Research Institute for Materials Science and Technology, Waseda University, 2-8-26 Nishiwaseda, Shinjuku-ku, Tokyo 169-0051, Japan

E-mail: miyata.hirokatsu@canon.co.jp, kuroda@waseda.jp

Abstract

Novel mesoporous TiO_2 films with regularly aligned slit-like nanovoids are prepared through structural transformation from a mesostructured TiO_2 film with honeycomb-packed aligned cylindrical micelles by pyrolytic removal of the micelle template. The transformation takes place through interconnection of the TiO_2 walls of the framework in the thickness direction by a heat-induced shrinkage and eventual collapse of the original channel structure. For the formation of this new structure, preparation of a mesostructured titania film with cylindrical micelles aligned entirely in the plane of the film over the whole thickness is indispensable. This is achieved by coating a substrate, on which a rubbing-treated polyimide layer is formed, with a precursor solution containing two nonionic surfactants, Brij56 and P123. In the mixed surfactant system, Brij56 works as an alignment-controlling agent through selective and directional adsorption on the anisotropic polymer surface. On the other hand, P123 suppresses the formation of a surface layer without controlled in-plane alignment, which has been inevitable when Brij56 are used alone. This is caused by the retarded condensation of the TiO_2 precursors due to increased coordination of oxyethylene moieties on titanium. P123 also increases the wall thickness of the framework, which also contributes to the formation of this mesoporous TiO_2 film with oriented regular

slit-like voids. The structural transformation takes place at a relatively low temperature range lower than 300 ^{o}C, which shows that the driving force is not crystallization. The mesoporous TiO_2 films with aligned slit-like voids shows optical anisotropy, birefringence, with a Δn value of ~0.023 reflecting the structural anisotropy of the film. Calcination of the aligned mesostructured TiO_2 film at 450 ^{o}C induces crystallization of TiO_2, which deteriorates the meso-scale structural regularity by interconnection of the TiO_2 walls. However, the partial retention of the regular structure is confirmed in the vicinity of the surface, which allows the retention of the optical anisotropy. The novel mesoporous TiO_2 films in this paper have a potential for optical applications by combining its unique anisotropic mesostructure, which enhances the accessibility to the inner surface, with various properties of TiO_2 such as high refractive index and photocatalytic activity.

Introduction

Nano-scale structural features of materials often develop various characteristic properties. Materials with nano-scale structural anisotropy can provide anisotropic properties, which are promising for applications to optical and electronic devices.[1,2] For practical applications, it is important that the structural features responsible for the desired properties are controlled over sufficient sizes, which are required for the

objective devices. When we bring out anisotropic properties originated from nano-scale structural anisotropy as device performances, the local structural anisotropy needs to be guaranteed over macroscopic scales.[3-15]

Mesostructured films prepared through self-assembly of surfactant molecules show various anisotropic properties when the structural anisotropy is provided on a macroscopic scale. The macroscopic orientation control of cylindrical mesochannels in mesostructured films and the consequent appearance of unique anisotropic properties have been extensively studied so far.[8-15] Many of the past researches are concerned with mesoporous silica films in which the anisotropy is provided by anisotropic accommodation of guest species into the aligned mesopores. However, variation of the materials that form the aligned mesopores should open up new possibilities based on the features of the materials. Especially, TiO_2 with high refractive index and photocatalytic activity is an attractive material and mesoporous TiO_2 films with cylindrical mesopores have been reported[16] including those with controlled pore orientation.[17] Recently, we reported the development of remarkable intrinsic birefringence of a TiO_2-based aligned mesoporous film.[8] The material of this film is a composite of TiO_2 and SiO_2, and therefore, the significant feature of TiO_2, high refractive index, is attenuated by the coexistent SiO_2. The complexation with silica is

indispensable for preventing the ordered structure from collapsing at the surfactant removal. Because of the low structural and adhesive stabilities of the mesostructured TiO_2 film with aligned two-dimensional (2D) hexagonal structure on a rubbed polyimide surface, removal of the template without losing the original structure has not been achieved although there are several reports on the advanced processes for template removal.[18-21] In the previous study, total alignment control over the entire thickness has also not been achieved, presumably due to the fast condensation rate of TiO_2 precursors. Here, we report total alignment control of cylindrical mesochannels in a mesostructured TiO_2 film, which transforms into anisotropic mesoporous TiO_2 films with aligned slit-like nanovoids by a thermal treatment. The original quasi 2D hexagonal structure collapses by removal of the surfactant, but the structural regularity in the plane of the film is retained by the interconnection of the vertical walls of the framework in the thickness direction. Although these films do not have regularly aligned cylindrical mesopores, they definitely have high structural anisotropy and mesoporosity. The slit-like shape provides better accessibility for guest species than cylindrical mesopores in conventional mesoporous films. Therefore, the film in this report will find many applications not only using its intrinsic anisotropy but also through complexation with various guest species.

Experimental Section

Preparation of mesoporous TiO_2 films with aligned slit-like nanovoids

Silicon substrates with a rubbing-treated poly(hexamethylenepyromellitimide) coating were prepared according to the same procedure as that in our previous paper,[22] except for the use of cotton instead of Nylon as the material of the buffing wheel. Brij56 (polyoxyethylene 10 cetylether) and P123 (polyethyleneoxide-polypropyleneoxide triblockcopolymer, PEO_{20}-PPO_{70}-PEO_{20}) were dissolved in 1-pentanol and then hydrochloric acid was added. Finally, titanium tetraisopropoxide (TTIP) was added with vigorous stirring, and the mixture was stirred for 1 h to prepare the precursor solution. The molar ratio of the final precursor solution was TTIP : 1-pentanol : HCl : H_2O : Brij56 : P123 = 1.0 : 15: 1.5 : 5.5 : 0.13 : 0.017. The substrate was coated with the precursor solution by spin-coating, and the obtained film was kept for 1 h in a 25 ^oC-60%RH atmosphere, followed by calcination at 250 ^oC, 350 ^oC and 450 ^oC for 4 h with a heating rate of 1 ^oC/min.

Characterization of mesostructured TiO_2 films

Scanning electron microscopy (SEM) was conducted with a Hitachi S5500 with an accelerating voltage of 2 kV. The two-dimensional (2D) X-ray diffraction (XRD)

patterns under the reflection mode with an incident angle of 0.2 ^{o} and the in-plane XRD patterns were recorded with a Rigaku ATX-G diffractometer using monochromated CuKα radiation. A 2D detector, Pilatus (Dextris) was used for recording the 2D-XRD patterns. The XRD patterns under the Bragg-Brentano geometry in a small angle region were recorded with a Rigaku Ultima IV diffractometer using FeKα radiation. The XRD in a high angle region for characterizing the TiO_2 crystallinity was performed with a Rigaku Ultima III diffractometer using CuKα radiation. Cross-sectional images of transmission electron microscopy (TEM) were recorded on a Hitachi H-800 at an accelerating voltage of 200 kV. Cross-sectional scanning TEM (STEM) images were recorded with a Tecnai F20 at an accelerating voltage of 200 kV in a high angle annular dark field (HAADF) mode. The specimens for cross-sectional TEM (STEM) observation were prepared by focused ion beam (FIB) process to thicknesses below 100 nm.

Optical measurements of the films

The optical anisotropy of the films was quantitatively characterized using a HAUP (high-accuracy universal polarimeter) method.[23-25] The monochromated light from a Xenon lamp with a wavelength of 550 nm was used. The sample films were placed between the crossed polarizers normal to the incident light, and the rotation angle of the

sample was set to the extinction position. Then, the transmittance was recorded with a photomultiplier as a function of the rotating angle of the second polarizer (analyzer). The Δn value was estimated using the HAUP theory and the film thickness was determined by cross-sectional SEM.

Results and Discussion

Preparation of mesostructured TiO_2 film with uniaxially aligned mesochannels

The XRD patterns of the as-deposited mesostructured TiO_2 film prepared on the rubbing-treated polyimide are shown in Fig. 1A (traces a and a'). Traces a and a' are recorded under a geometry wherein the projection of the incident X-rays on the film

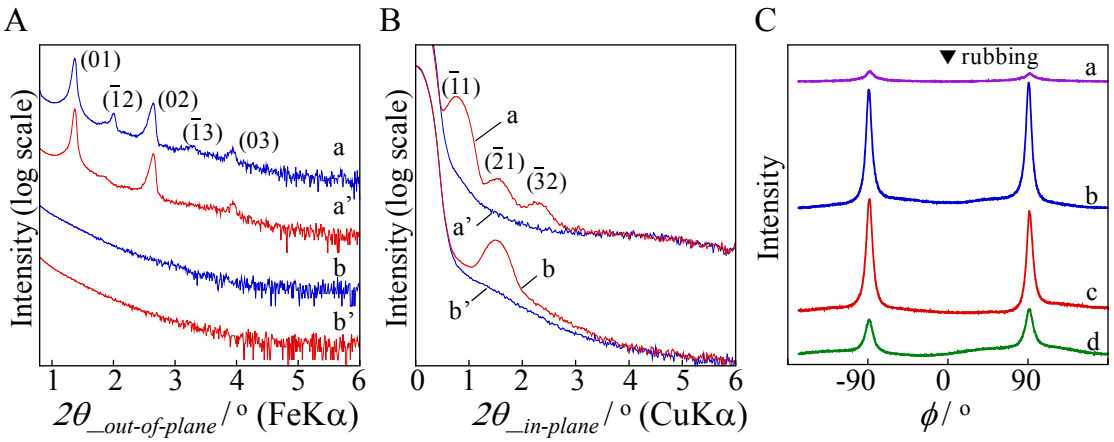

Fig. 1. XRD patterns of the mesostructured TiO_2 films. XRD patterns recorded under the A: Bragg-Brentano and B: in-plane geometries. Traces a, a': before and b, b': after calcination at 350 °C. The projected direction of the incident X-rays on the film is perpendicular (a, b) and parallel (a', b') to the rubbing direction. C: In-plane rocking curves for ($\bar{2}$ 1) plane: before (a) and after calcination at 250 °C (b), 350 °C (c), 450 °C (d).

surface is perpendicular and parallel to the rubbing direction, respectively. The intensity is shown on a log scale to display all the diffraction peaks with different intensities at once. Five diffraction peaks are confirmed under the perpendicular geometry, whereas the number of the evident peaks is three under the parallel geometry. The observed difference undoubtedly comes from the structural anisotropy in the plane of the film, and these observed patterns are consistent with a uniaxially aligned 2D-hexagonal structure, which has been successfully formed for mesostructured silica films using the same substrate with a rubbing-treated polyimide coating,[22,26] The lattice planes ($\bar{1}$ 2) and ($\bar{1}$ 3) are not parallel to the substrate surface, and therefore, do not satisfy the diffraction condition under the ideal Bragg-Brentano geometry. However, the broadened reciprocal lattice points of mesostructured materials, which appear in the low-angle region, and finite divergence angle of X-rays make these spots detectable. These spots are not observed when the incident X-rays are perpendicular to the mesochannels. Such an anisotropic appearance of these spots is the evidence of the controlled in-plane alignment of the mesochannels.

The d_{01} value of the film is estimated to be 8.3 nm, taking into account the refraction of the X-rays at the surface. This value is much larger than that of the 2D-hexagonal mesostructured TiO_2 film with an imperfect alignment, which is prepared using Brij56

alone on the same polyimide substrate.[8] This large periodicity is due to the increase of the size of the micelles by using a bulky block copolymer surfactant, P123. It must be noted that the use of P123 alone does not provide an aligned mesostructure on the rubbing-treated polyimide.[27] This is presumably due to insufficient interfacial interactions between the oriented polyimide chains on the substrate and the hydrophobic polypropyleneoxide block for the total alignment of micelles. However, as described above, in-plane alignment of the micelles, which are dominantly consisting of block copolymers, in a mesostructured TiO_2 film can be controlled with a help of Brij56. It is considered that Brij56 works as an alignment controlling agent through strong hydrophobic interactions between its alkyl group and the aligned polyimide chains, as we recently reported for mesostructured silica films.[27]

The in-plane alignment of the micelles is quantitatively evaluated by in-plane XRD. As shown in Fig. 1B, three diffraction peaks, which are assigned to ($\bar{1}$ 1), ($\bar{2}$ 1) and ($\bar{3}$ 2) of a 2D-hexagonal structure, are observed when the projection of the incident X-rays are perpendicular to the rubbing direction at ϕ (sample rotation angle) = 0^o (trace a). Because of the intrinsically weak diffraction intensity of ($\bar{2}$ 1), this peak is observed only when the structural regularity is considerably high. In our previous study, this peak was not observed for the mesostructured TiO_2 film prepared using Brij56 alone

due to its inferior uniformity regardless of the controlled in-plane alignment.[8] On the other hand, no diffraction peaks are observed under the parallel geometry (Fig. 1B trace a'), which indicates complete alignment of the mesochannels. The in-plane ϕ-scanning profile for the ($\bar{2}$ 1) peak proves the uniaxial alignment of the mesochannels perpendicular to the rubbing direction with a narrow distribution of the alignment direction (Fig. 1C trace a). The distribution of the alignment represented by the full-width at half maximum of the ϕ-scanning profiles with respect to the ($\bar{2}$ 1) and ($\bar{1}$ 1) peaks are estimated to be 11.7 ^{o} and 8.4 ^{o}, respectively (Fig. S1†). This distribution of the alignment direction is comparable with that of the aligned mesostructured silica film with a similar (01) spacing of 8.0 nm in our previous report,[27] which film was also prepared using a mixture of P123 and Brij56. The use of this surfactant mixture enables the preparation of highly aligned nonsiliceous mesostructured films, which have regularity comparable with that of aligned mesostructured silica films, on the basis of common chemistry irrespective of large differences in the condensation rate.

The complete alignment over the whole thickness of the film is finally evidenced by cross-sectional TEM and STEM, as shown in Fig. 2A and 2B. The surface layer without a controlled in-plane alignment, which is inevitably formed on the top of the aligned film when Brij56 is used alone,[8] was not observed. This surface layer is

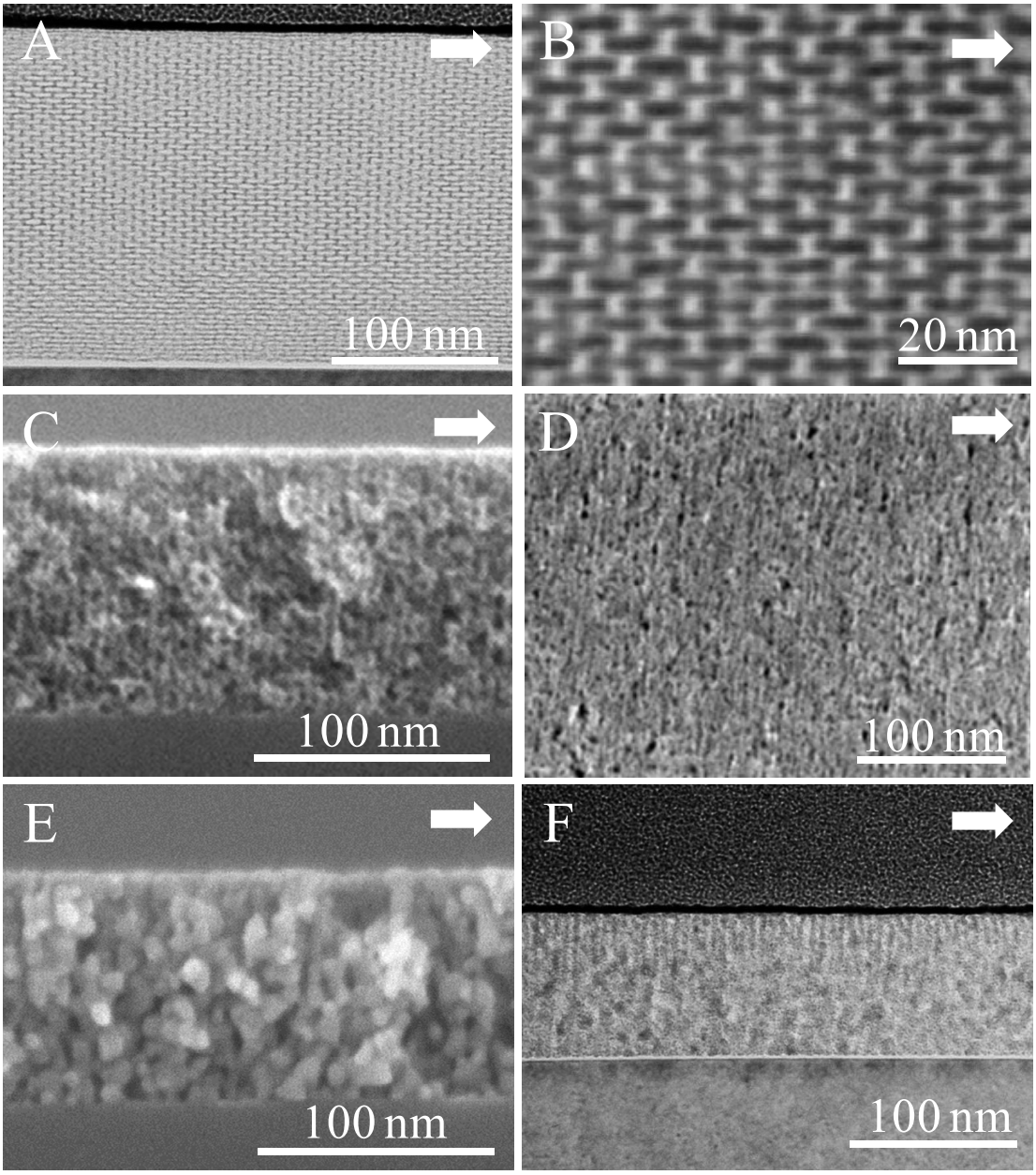

Fig. 2. Electron micrographs of the mesostructured TiO_2 films. A: TEM and B: STEM image of the cross-section of the as-deposited film, C: cross-sectional SEM image of the film calcined at 350 ^{o}C, D: top-view SEM image of the film calcined at 250 ^{o}C, E: SEM and F: TEM image of the cross-section of the film calcined at 450 ^{o}C. White arrows show the rubbing direction.

unfavorably formed from the air interface probably due to the fast condensation rate of the titania precursors. The absence of the non-aligned surface layer means that the

structure of the film in this report has been fixed unidirectionally from the anisotropic substrate surface. This is evidently caused by the added P123, which should retard the condensation rate of the titania precursors due to the increased coordination of the oxyethylene moieties on titanium.[28-30] Nobody has succeeded in the preparation of entirely aligned nonsiliceous mesostructured films, for which development of novel functionalities are expected. Therefore, the method in this paper brings a significant progress not only in the preparation techniques but also in the applicability of mesostructured materials.

Evidently, the hexagonal structure is largely distorted, and the cross-section of each mesochannel is deformed to a rectangular shape (Fig. 2A, 2B). This is inconsistent with the XRD results, which show that the deviation from an ideal hexagonal structure is less than 20%. This inconsistency can be explained by the vertical shrinkage of the film by the electron beam irradiation in the courses of the specimen preparation and observation of the images. The STEM image provides more detailed structural information. As can be seen from Fig. 2B, the vertical channel walls are apparently thicker than those in the other directions. This can also be explained by the unidirectional shrinkage along the thickness direction. The observed large shrinkage by an electron beam damage has not been observed for aligned mesostructured silica

films prepared by dip-coating,[31] which indicates the inferior structural stability of the mesostructured TiO_2 film.

Structural changes by pyrolytic removal of the surfactants

In our previous study, we found that the regular 2D-hexagonal structure of a mesostructured TiO_2 film prepared using Brij56 completely collapses upon surfactant removal by a thermal treatment.[8] Although the thickness of the channel wall somewhat increases by mixing of P123, the large shrinkage upon electron beam irradiation indicates inferior structural stability compared to siliceous materials. As expected, the calcined films give no diffraction peaks under the Bragg-Brentano geometry, irrespective of the directional relationship between the rubbing treatment and the incident X-rays (Fig. 1A traces b, b'). The structural periodicity along the thickness direction cannot be retained even when the calcination temperature is reduced to 250 ^{o}C, which is much lower than the crystallization temperature of TiO_2. Actually, no XRD peaks are observed in the wide angle region, which proves the amorphous nature of TiO_2. This shows that the observed collapse of the 2D-hexagonal structure is not caused by crystallization of the pore walls.

Because XRD under the Bragg-Brentano geometry predominantly gives the structural information of the lattice planes parallel to the substrate, the observed disappearance of

the diffraction peaks does not sufficiently prove the complete loss of the periodic structure. For example, a 2D-hexagonal film with a $<\bar{2}\,1>$ orientation does not provide a principal diffraction peak in the XRD patterns taken with the Bragg-Brentano geometry, as we reported recently.[32] Therefore, we measured the 2D-XRD patterns of the films.[33] Figure 3 shows the change of the 2D-XRD patterns of the film by calcination at 450 ^{o}C. The patterns A and C, B and D are recorded under the geometry wherein the projection of the incident X-rays on the film is perpendicular and parallel to the rubbing direction, respectively. The loss of the periodic structure along the thickness direction is confirmed by the absence of the (01) spot in Fig. 3C and 3D. However, the $(\bar{2}\,1)$ spot is still observed, as shown in Fig. 3C (yellow dotted circle). This proves that the structural periodicity in the plane of the film is retained to some extent even after the high temperature treatment. The formation of a mesoporous TiO_2 film with a regular grid-like in-plane structure by thermal treatment of a cubic mesostructured TiO_2 film has been reported.[34,35] However, survival of the in-plane structural regularity with respect to a 2D-hexagonal mesostructured TiO_2 film with a mechanically weaker framework is achieved for the first time. This is quite important because it suggests the possibility of general formation of anisotropic mesoporous films even with materials whose stability is too low to keep the original mesostructure at

pyrolytic removal of the templates.

To investigate the in-plane structural regularity of the film after the surfactant removal, we performed detailed in-plane XRD study, as shown in Fig. 1B and C. The trace b and b' in Fig. 1B clearly demonstrate that only the in-plane structural regularity is retained after the surfactant removal. The position of the ($\bar{2}$ 1) peak is unchanged, showing that the lattice distance in the plane of the film is kept constant value of 5.9 nm.

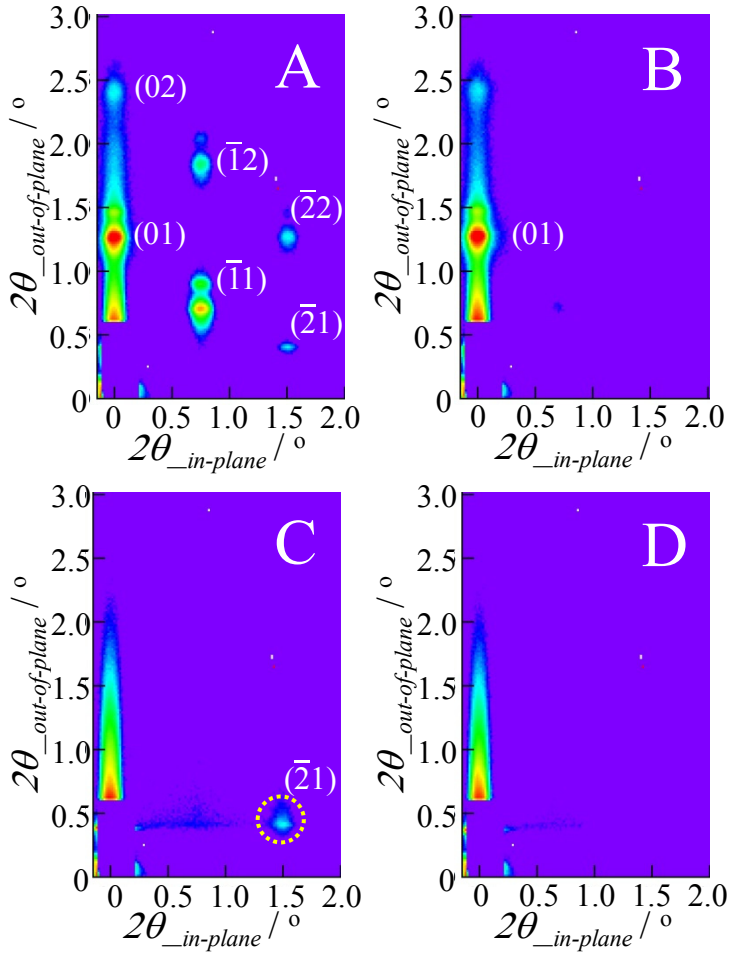

Fig. 3. 2D XRD patterns of the mesostructured titania film before (A, B) and after calcination at 450 °C (C, D). The projected direction of the incident X-rays on the film is perpendicular (A, C) and parallel (B, D) to the rubbing direction.

The increase of the diffraction intensity is explained by the considerable retention of the structural regularity in the lateral direction and improvement of the X-ray scattering efficiency, which is caused by the replacement of the surfactant with air. The in-plane rocking curves for the ($\bar{2}$ 1) peak recorded for the films calcined at different temperatures are shown in Fig. 1C (traces b-c). The films calcined at 250 ^{o}C and 350 ^{o}C give almost the same profile, showing the structure of the film does not change when the calcination temperature increases from 250 ^{o}C to 350 ^{o}C. It should be noted that TiO_2 is still amorphous after the thermal treatment at 350 ^{o}C. The peak width of the in-plane rocking curve is not broadened after 350 ^{o}C annealing, which suggests that the structural anisotropy is not influenced by the drastic structural transformation as long as crystallization does not take place.

The retention of the structural regularity in the plane of the film after 350 ^{o}C calcination is also confirmed by SEM. The parallel stripes with a constant interval observed in Fig. 2C show the formation of aligned slit-like nanovoids and are direct evidence of the retention of the structural regularity in the plane of the film, which is consistent with the in-plane XRD results. Thus, the formation of a mesoporous TiO_2 film with regularly aligned slit-like nanovoids is confirmed. The slit-like voids are confirmed also in the top-view image of the film, as shown in Fig. 2D. We performed

fast Fourier transformation (FFT) for Fig. 2(D) and compared the profiles along the directions parallel and normal to the alignment direction of the mesopores. The difference of the profiles is consistent with the aligned regular mesostructure (Fig. S2†), which means that the aligned slit-like mesoporous structure is confirmed by this SEM image. The anisotropic shape of the nanovoids gets less remarkable with the increase of the calcinations temperature (Fig. S3†), due to interconnection of the pore walls. Because the top surface of a mesostructured film with a 2D-hexagonal structure is covered with a continuous inorganic layer without openings, the slit-like shape is not so evident as those reported for the film transformed from a cubic structure.[35] Although the parallel stripes are confirmed in the cross-sectional images, the slit-like shape of the nonavoids is not very clear. It is considered that the TiO_2 pore walls consisting the slit-like nanovoids are partially interconnected, reflecting the original mesostructure, keeping the average interplanar distance constant.

The structure of the film significantly changes when the calcination temperature increases to 450 ^{o}C because of crystallization of TiO_2. The regular stripes, which are observed for the films calcined at lower temperatures (250 ^{o}C and 350 ^{o}C), are not observed but aggregated particles with a diameter smaller than 10 nm is confirmed instead (Fig. 2E). The XRD pattern in the wide-angle region recorded for the film

after 450 °C calcination is shown in Fig. 4A, which confirms the formation of anatase nanocrystals. The crystallite size was estimated to be 8.2 nm from the width of the (101) diffraction peak using the Scherrer's formula. This is quite consistent with the grain size in the SEM image.

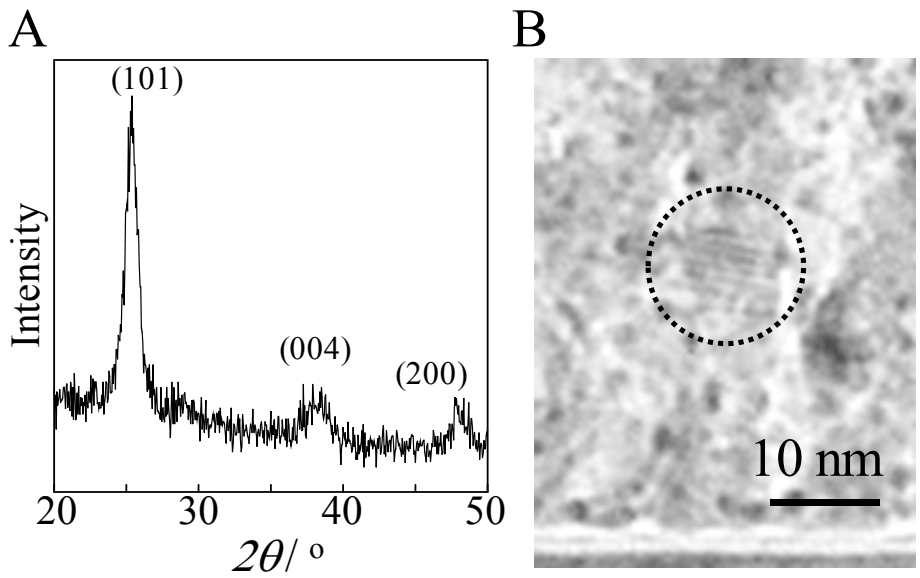

Fig. 4. XRD pattern of the wide-angle region (A) and high-magnification TEM image (B) of the film calcined at 450 °C. The moiré pattern in the dotted circle in (B) shows the existence of the microscopic TiO_2 crystals.

In spite of such large structural change caused by crystallization, the original mesostructure is still partially retained, which is confirmed by the existence of a clear diffraction peak caused by the in-plane structural regularity (Fig. 1C, trace d). The cross-sectional TEM unveiled the real structure of the film wherein both the anatase nanocrystals and aligned slit-like voids are involved. In the cross-sectional TEM image, Fig. 2F, regular stripes are confirmed only in the vicinity of the film surface, and

a granular texture is observed over the half thickness of the film on the substrate side. This shows that the walls of the mesoporous TiO_2 film with slit-like nanovoids are interconnected to form nanoscale grains except for the regions in the vicinity of the surface, wherein the original mesoporous structure is retained. The interconnection of the TiO_2 walls can also be confirmed by the moiré pattern in the high magnification TEM image (Fig. 4B). The domain size where the moiré pattern is observed is larger than the wall thickness, which is the direct evidence of the interconnection of the TiO_2 walls.

The thickness of the film after 450 ^oC calcination is about 90 nm, which is less than half of that of the film before calcination. This is consistent with the total collapse of the porous structure in the thickness direction, which is predicted from XRD. Regardless of such large shrinkage of the film, the calcined film does not have macroscopic cracks. This is because of the release of the stress in the plane of the film through the microscopic splitting of the film by the formation of the slit-like nanovoids. The formation of crystalline mesoporous film with distinct structural anisotropy will also prompt new applications.

Optical anisotropy of the calcined mesoporous TiO_2 films with slit-like nanovoids

Because of this anisotropic meso-scale structure consisting of TiO_2 and air, the films

after calcination show optical birefringence. The Δn value is estimated to be 0.023 at λ = 550 nm for both of the films calcined at 250 °C and 350 °C. This indicates that the structure of the film is almost unchanged when the calcination temperature increases from 250 °C to 350 °C. Although the regular 2D hexagonal structure is collapsed by the surfactant removal by a thermal treatment, development of anisotropic optical property originated from the retained lateral structural anisotropy is thus achieved. Such an anisotropic film cannot be obtained when the mesostructured TiO_2 film is prepared using P123 alone because of the lack of in-plane alignment. Also, the use of Brij56 alone does not provide evident optical anisotropy because anisotropic structure is completely lost by calcination.

It should be noted that the Δn value estimated for the film calcined at 450 °C is almost the same as those estimated for the films calcined at lower temperatures. This seems to be strange because crystallization evidently deteriorates the aligned mesoporous structure, though the in-plane XRD rocking curve (Fig. 1C trace d) suggests partial retention of the structural anisotropy. This can be explained by increase of the refractive index of TiO_2 by crystallization and consequent increase of Δn. It is considered that the increase of Δn value by crystallization compensates the decrease of the value by degradation of the anisotropic structure.

The estimated Δn values are much lower than those expected from calculation for aligned mesoporous TiO_2 films.[8] This would be due to the imperfection of the slit-like nanovoids in the films. It is considered that the TiO_2 walls are not completely separated by the slit-like nanovoids but partially interconnected laterally reflecting the original 2D-hexagonal structure. However, it is necessary to increase the Δn value for practical application of these films to optical elements such as phase plates, which require much larger optical retardation. Increase of the structural periodicity of the original mesostructured TiO_2 film with an aligned 2D-hexagonal structure would be a breakthrough for this requirement. If the lateral distance becomes larger, the TiO_2 walls that form the slit-like nanovoids would be more isolated. It may suppress even the interconnection at the crystallization process, which further increases the birefringence.

Formation mechanism of mesoporous TiO_2 films with aligned slit-like nanovoids

The most plausible explanation for the formation mechanism of the mesoporous TiO_2 film with slit-like nanovoids is the interconnection of the vertical wall of the framework in the thickness direction during the heat treatment (Fig. 5). This hypothesis is based on the cross-sectional TEM and STEM images of the film before calcination shown in Fig. 2A and 2B. As can be seen in the images, the cross-section of the mesochannels

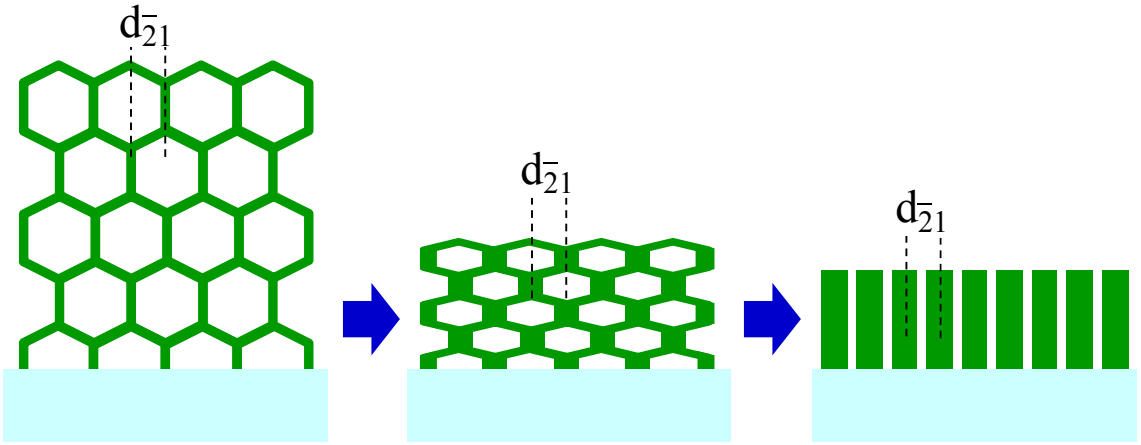

Fig. 5. Schematic illustration of the transformation mechanism of the mesostructured TiO_2 film from the aligned 2D-hexagonal structure to the slit-like nanovoid arrays by pyrolytic surfactant removal.

becomes almost rectangular by the electron-beam-induced large shrinkage of the film in the thickness direction. Also, the TiO_2 walls normal to the substrate surface increase their thickness and are aligned with a uniform interval. The pyrolytic surfactant removal results in the total collapse of the cylindrical mesochannels leaving regularly aligned plate-like thin TiO_2 walls, which are formed through vertical interconnection of the walls of the original framework. The distance of the adjacent slit-like nanovoids in the film after this transformation is just half of the lateral inter-micelle distance of the original 2D-hexagonal film because of the retention of the $(\bar{2}\,1)$ spacing. As explained above, the formation of the slit-like nanovoids is ascribed to the interconnection of the wall, which is different from the appearance of a vertical porosity through interconnection of the spherical mesopores.[18,36,37] When Brij56 is used alone

for the preparation of the aligned mesostructured TiO_2 film, the formation of such slit-like nanovoids is not confirmed. This would be due to the lower thermal stability of the framework prepared using Brij56. It is known that the use of PEO-b-PPO-b-PEO triblock copolymers such as P123 allows the formation of mesostructured materials with larger wall thicknesses.[38] In the present case, it is likely that the increased wall thickness prevents the mesostructure from totally collapsing by pyrolytic surfactant removal.

Conclusion

A mesostructured TiO_2 film with an entirely aligned 2D-hexagonal structure, which is prepared on a rubbing-treated polyimide film using a surfactant mixture of P123 and Brij56, is transformed into a novel mesoporous TiO_2 film with regularly aligned slit-like nanovoids by pyrolytic removal of the surfactants at a temperature range wherein crystallization does not take place. This unique structure is formed by interconnection of the framework in the thickness direction, which is accompanied by the total collapse of the original 2D-hexagonal structure. The obtained films show remarkable birefringence with a Δn value of 0.023, which is originated from the highly anisotropic porous structure. Crystallization of TiO_2 by increasing the calcination temperature to 450 ^{o}C results in the eventual formation of TiO_2 nanocrystals. Although this lowers

the structural regularity, the partial retention of the anisotropic structure in the vicinity of the surface allows the retention of the optical anisotropy. The TiO_2 film with a novel mesoporous structure in this report is expected to find useful applications by combining their unique structural anisotropy and various properties of TiO_2. The formation of anisotropic mesoporous films via the meso-scale structural transformation reported in this paper would be possible with other nonsiliceous materials, which will further increase opportunity of application of anisotropic mesoporous films.

Acknowledgement

The authors acknowledge Dr. Alexis Debray (Canon Inc.) for careful reviewing of the manuscript. The authors thank Dr. W. Kubo (Canon Inc.) for the 2D-XRD measurement. The authors acknowledge Prof. T. Asahi (Waseda Univ.) for optical measurements.

† Electronic supplementary information (ESI) available: In-plane rocking curves for ($\overline{2}$ 1) and ($\overline{1}$ 1) planes recorded for the mesostructured TiO_2 film before calcination, FFT analysis for the surface SEM image of the mesoporous TiO_2 film calcined at 250 ^{o}C, top view SEM images of the mesoporous TiO_2 film calcined at 350 ^{o}C. See DOI:

References

1. *Anisotropic Nanomaterials*, ed. L. M. Liz-Marzán, Themed Collections of *J. Mater. Chem.*; Royal Society of Chemistry: London, 2006; vol. 11, pp. 3877-3984.

2. P. R. Sajanlal, T. S. Sreeprasad, A. K. Samal, T. Pradeep, *Nano Rev.* 2011, *2*: 5883 - DOI: 10.3402/nano.v2i0.5883.

3. M. Yoshino, T. Kagata, K. Hoshino, T. Mukai, H. Ohno, T. Kato, *J. Am. Chem. Soc.*, 2006, *128*, 5570.

4. P. W. Majewski, M. Gopinadhan, W.-S. Jang, J. L. Lutkenhaus, C. O. Osuji, *J. Am. Chem. Soc.*, 2010, **132**, 17516.

5. J. Li, K. Kamata, M. Komura, T. Yamada, H. Yoshida, T. Iyoda, *Macromolecules*, 2007, **40**, 8125.

6. S. Hong, J. Huh, X. Gu, D. H. Lee, W. H. Jo, S. Park, T. Xu, T. P. Russel, *Proc. Natl. Acad. Sci. U.S.A.*, 2012, **109**, 1402.

7. Q. Liu, Y. Cui, D. Gardner, X. Li, S. He, I. I. Smalyukh, *Nano Lett.,* 2010, **10**, 1347.

8. H. Miyata, Y. Fukushima, K. Okamoto, M. Takahashi, M. Watanabe, W. Kubo, A. Komoto, S. Kitamura, Y. Kanno, K. Kuroda, *J. Am. Chem. Soc.*, 2011, **133**, 13539.

9. T. Suzuki, H. Miyata, T. Noma, K. Kuroda, *J. Phys. Chem. C*, 2008**, 112***,* 1831.

10. W. C. Molenkamp, M. Watanabe, H. Miyata, S. H. Tolbert, *J. Am. Chem. Soc.*, 2004,

126, 4476.

11. W. Cui, X. Lu, B. Su, Q. Lu, Y. Wei, *Appl. Phys. Lett.*, 2009, **95**, 153102.

12. R. L. Rice, D. C. Arnold, M. T. Shaw, D. Iacopina, A. J. Quinn, H. Amenitsch, J. D. Holmes, M. A. Morris, *Adv. Func. Mater.*, 2007, **17**, 133.

13. G. Kawamura, I. Hayashi, H. Muto, A. Matsuda, *Scripta Mater.*, 2012, **66**, 479.

14. I. B. Martini, I. M. Craig, W. C. Molenkamp, H. Miyata, S. H. Tolbert, B. J. Schwartz, *Nat. Nanotechnol.*, 2007, **2**, 647.

15. H. Fukumoto, S. Nagano, T. Seki, *Chem. Lett.*, 2006, **35**, 180.

16. M. J. Q. Yong, A. S. W. Wong, G. W. Ho, *Mater. Chem. Phys.*, 2009, **63**, 1624.

17. F. Shan, X. Lu, Q. Zhang, J. Wu, Y. Wang, F. Bian, Q. Lu, Z. Fei, P. J. Dyson, *J. Am. Chem. Soc.*, 2012, **134**, 20238.

18. D. Grosso, G. J. A. A. Soler-Illia, E. L. Crepaldi, F. Cagnol, C. Sinturel, A. Bourgeois, A. Brunet-Bruneau, H. Amenitsch, P.-A. Albouy, C. Sanchez, *Chem. Mater.*, 2003, **15**, 4562.

19. K. Cassiers, T. Linssen, V. Meynen, P. Van Der Voort, P. Cool and E. F. Vansant, *Chem. Commun.*, 2003, 1178.

20. K. Wang, M. A. Morris, J. D. Holmes, *Chem. Mater.*, 2005, **17**, 1269.

21. K. Wang, B. Yao, M. A. Morris, J. D. Holmes, *Chem. Mater.*, 2005, **17**, 4825.

22. H. Miyata, T. Noma, M. Watanabe, K. Kuroda, *Chem. Mater.*, 2002, **14**, 766.

23. J. Kobayashi, Y. Uesu, *J. Appl. Cryst.*, 1983, **16**, 204.

24. W. Weiglhofer, A. Lakhtakia, *Introduction to Complex Mediums for Optics and Electromagnetics*; SPIE Press, Washington, 2003.

25. M. Tanaka, N. Nakamura, H. Koshima, T. Asahi, *J. Phys. D: Appl. Phys.* 2012, **45**, 175303.

26. A. Komoto, W. Kubo, H. Miyata, *Chem. Lett.*, 2012, **41**, 741.

27. S. Hayase, Y. Kanno, M. Watanabe, M. Takahashi, K. Kuroda, H. Miyata, *Langmuir*, 2013, **29**, 7096.

28. P. Yang, D. Zhao, D. I. Margolese, B. F. Chmelka, G. D. Stucky, *Chem. Mater.*, 1999, **11**, 2813.

29. G. J. A. A. Soler-Illia, C. Sanchez, *New J. Chem.*, 2000, **24**, 493.

30. G. J. A. A. Soler-Illia, P. C. Angelomé, M. C. Fuertes, D. Grosso, C. Boissiere, *Nanoscale*, 2012, **4**, 2549.

31. H. Miyata, Y. Kawashima, M. Itoh, M. Watanabe, *Chem. Mater.*, 2005, **17**, 5323.

32. H. Miyata, S. Kobori, W. Kubo, M. Watanabe, K. Kuroda, *Langmuir,* 2013, **29**, 761.

33. T. Noma, K. Takada, H. Miyata, A. Iida, *Nucl. Instrum. and Methods in Phys. Res. A*, 2001, **467-468**, 1021.

34. Y. Sakatani, D. Grosso, L. Nicole, C. Boissière, G. J. A. A. Soler-Illia, C. Sanchez, *J. Mater. Chem.*, 2006, **16**, 77.

35. I. L. Violi, M. D. Perez, M. C. Fuertes, G. J. A. A. Soler-Illia, *ACS Appl. Mater. Interfaces*, 2012, **4**, 4320-4330.

36. C.-W. Wu, T. Ohsuna, M. Kuwabara, K. Kuroda, *J. Am. Chem. Soc.*, 2006, **128**, 4544.

37. H. Oveisi, X. Jiang, M. Imura, Y. Nemoto, Y. Sakamoto, Y. Yamauchi, *Angew. Chem. Int. Ed.*, 2011, **50**, 7410.

38. G. J. A. A. Soler-Illia, E. Scolan, A. Louis, P.-A. Albouy, C. Sanchez, *New J. Chem.*, 2001, **25**, 156.

Figure Captions

Fig. 1. XRD patterns of the mesostructured TiO_2 films. XRD patterns recorded under the A: Bragg-Brentano and B: in-plane geometries. Traces a, a': before and b, b': after calcination at 350 ^oC. The projected direction of the incident X-rays on the film is perpendicular (a, b) and parallel (a', b') to the rubbing direction. C: In-plane rocking curves for ($\bar{2}$ 1) plane: before (a) and after calcination at 250 ^oC (b), 350 ^oC (c), 450 ^oC (d).

Fig. 2. Electron micrographs of the mesostructured TiO_2 films. A: TEM and B: STEM

image of the cross-section of the as-deposited film, C: cross-sectional SEM image of the film calcined at 350 ^{o}C, D: top-view SEM image of the film calcined at 250 ^{o}C, E: SEM and F: TEM image of the cross-section of the film calcined at 450 ^{o}C. White arrows show the rubbing direction.

Fig. 3. 2D XRD patterns of the mesostructured titania film before (A, B) and after calcination at 450 ^{o}C (C, D). The projected direction of the incident X-rays on the film is perpendicular (A, C) and parallel (B, D) to the rubbing direction.

Fig. 4. XRD pattern of the wide-angle region (A) and high-magnification TEM image (B) of the film calcined at 450 ^{o}C. The moiré pattern in the dotted circle in (B) shows the existence of the microscopic TiO_2 crystals.

Fig. 5. Schematic illustration of the transformation mechanism of the mesostructured TiO_2 film from the aligned 2D-hexagonal structure to the slit-like nanovoid arrays by pyrolytic surfactant removal.

Table of contents entry

Mesoporous TiO_2 films with aligned slit-like nanovoids is formed by calcination of a fully aligned mesostructured TiO_2 film.